

## Partial Hessian Vibrational Analysis of Organic Molecules Adsorbed on Si(100)

Nicholas A. Besley\* and James A. Bryan

School of Chemistry, University of Nottingham, University Park, Nottingham, NG7 2RD United Kingdom

Received: August 2, 2007; In Final Form: November 21, 2007

A partial Hessian approach is used to study the vibrational spectroscopy of acetylene, ethylene, benzene, 1,3-butadiene, and naphthalene adsorbed on the Si(100) surface. The partial Hessian approximation introduces a very small error in the computed frequencies and intensities of the adsorbed molecules and results in a significant reduction in computational cost. Exploiting this reduced computational cost, molecular adsorbates on large cluster models of the Si(100) surface can be studied with density functional theory. Using clusters with two and four silicon–silicon dimers, the effects of surface coverage and the spectroscopy of large adsorbates that bind to more than one dimer are studied. For benzene and butadiene, molecules adsorbed on neighboring silicon dimers in the same dimer row can have a significant effect on the infrared spectrum in the C–H stretching region, changing both the frequency and intensity of the computed vibrational modes. A weaker effect is observed for molecules adsorbed in adjacent dimer rows. Comparison of the computed spectra with experiment shows that several binding configurations are present for benzene. For 1,3-butadiene, the adsorption product is dominated by the product of a Diels–Alder [4+2] addition. However, the product may have the hydrogens of the  $sp^2$  carbons cis or trans with respect to each other. Larger cluster models of the surface also allow large adsorbates that can bind to multiple silicon dimers to be studied. The infrared spectroscopy of naphthalene bound to one, two, and four silicon dimers is computed. Comparison with experiment shows that naphthalene preferentially binds within a dimer row.

### Introduction

There is currently considerable interest in organic functionalization of semiconductor surfaces. One of the key reasons for this growing interest is the potential importance of these systems in the development of new semiconductor based devices.<sup>1</sup> The Si(100) surface lies at the heart of much of this work. The Si(100) surface undergoes a characteristic ( $2 \times 1$ ) reconstruction in which adjacent atoms pair, and the resulting silicon dimers make the surface particularly amenable to organic functionalization. The adsorption of a wide range of organic molecules on the Si(100) surface have been studied through both experiment and theory, for examples see references<sup>2–8</sup> Organic molecules with  $\pi$  bonds react with the surface to form C–Si  $\sigma$  bonds. Larger hydrocarbons containing several unsaturated carbon–carbon bonds can react with the surface resulting in many configurations of the surface adsorbed species. Understanding and controlling the adsorption of such molecules is central to the development of these technologies. Spectroscopic techniques can probe the structure of the adsorbed molecules. Recently, we have developed theoretical approaches to study the spectroscopy of molecules adsorbed on surfaces,<sup>9,10</sup> including the electronic<sup>11</sup> and near-edge X-ray absorption fine structure<sup>12</sup> spectroscopies of organic molecules on Si(100). Such calculations can play an important role in their structural characterization since they provide a direct link between a structure predicted by theory and the structure observed in experiment.

Infrared (IR) spectroscopy is a particularly sensitive technique and can be used to distinguish between different adsorption configurations. Bent and co-workers have studied the adsorption of a range of organic molecules including benzene, 1,3-butadiene, 2,3-dimethyl-1,3-butadiene, and amines on Si(100) with multiple internal reflection IR spectroscopy.<sup>13–16</sup> Once adsorbed on the surface, benzene showed two distinct vibrational

features at 2045 and 3044  $cm^{-1}$ , which were assigned to the C–H stretching frequencies of the  $sp^3$  and  $sp^2$  hybridized carbons, respectively.<sup>14</sup> This was consistent with earlier work at lower resolution that observed two broad features at 2935 and 3065  $cm^{-1}$ .<sup>17</sup> Another study showed several C–H stretching modes, ranging in frequency from 2899 to 3043  $cm^{-1}$ .<sup>18</sup> The dominant adsorbed structure was shown to arise from a Diels–Alder [4+2] addition to form a 1,4-cyclohexadiene like structure. The Diels–Alder product was also found to be favored by 1,3-butadiene and 2,3-dimethyl-1,3-butadiene.<sup>13</sup> The addition of 2,3-dimethyl-1,3-butadiene to Si(100) was also explored by Hamers and co-workers.<sup>19</sup> The surface species were found to comprise 80% of the Diels–Alder product, with the remaining 20% arising from a [2+2] addition. Okamura et al.<sup>20</sup> used IR spectroscopy to investigate the adsorption of naphthalene on Si(100). Their results showed that the binding of naphthalene to the surface is dependent on surface coverage. At low coverage, the dominant configuration was found to correspond to naphthalene bonded to two silicon dimers in the same row. At high coverage, several binding configurations were present.

Calculations of the vibrational frequencies of molecules adsorbed on Si(100) have also been reported. Konecny and Doren reported C–H stretching frequencies of 1,3-butadiene and 2,3-dimethyl-1,3-butadiene. The calculations used a  $Si_9H_{12}$  cluster model of the surface in conjunction with density functional theory (DFT).<sup>21,22</sup> The calculations indicated that the [4+2] and [2+2] reaction products could be distinguished, and the predicted spectra for the Diels–Alder product was consistent with experiment. Lopinski et al. used a larger cluster model of the surface with the semiempirical Austin method 1 (AM1) approach to study the vibrational frequencies of benzene on Si(100).<sup>18</sup> Comparison with experiment indicated that benzene adopted multiple binding configurations. DFT calculations with

the  $\text{Si}_9\text{H}_{12}$  cluster have also been used to study the vibrational frequencies of cyclopentadiene and methylamine.<sup>16,23</sup> A combination of experiment and DFT was used to investigate the IR spectroscopy of octasilasesquioxane ( $\text{H}_8\text{Si}_8\text{O}_{12}$ ) on the surface.<sup>24</sup> More recently, Okamura et al.<sup>20</sup> used DFT to compute IR spectra for naphthalene bound to one and two silicon dimers. In addition, the effect of the interaction between two adsorbed naphthalene molecules on the IR spectra was examined in order to account for the dependence on surface coverage observed in experiment. Generally, the calculation of the vibrational frequencies of adsorbed molecules use small clusters to model the silicon surface. For small adsorbates these models may be sufficient. However, for larger molecules that can bind to more than one silicon dimer, larger cluster models of the surface are required. Pursuing such calculations is restricted by the rise in computational cost. In order to achieve calculations of large adsorbates with extensive cluster models of the surface, techniques that reduce the cost of these calculations are required.

Vibrational frequency calculations usually adopt the harmonic approximation. Within this approximation, frequencies and normal coordinates are obtained from the diagonalization of the mass-weighted Hessian matrix. The computational cost of finding pre-selected vibrational modes can be reduced through the mode-tracking approach.<sup>25,26</sup> Using a suitable estimate of the normal mode, an iterative Davidson algorithm is used to construct the exact normal mode and frequency. This approach has been used to compute the vibrational spectrum of thiophenolate anion on a  $\text{Ag}_{51}$  cluster.<sup>25</sup> For this problem, the computational effort was reduced by 20–30%. The advantage of this approach is that it provides the exact frequencies (within the theoretical model) since it does not approximate the Hessian. Alternatively, a partial Hessian approach provides an intuitive approach to reduce the cost of these calculations. Early work using this method was reported by Head.<sup>27–29</sup> Generally in a partial Hessian approach, only the adsorbate block of the Hessian matrix is computed and diagonalized, greatly reducing the computational cost of the calculation. Physically, this corresponds to assigning an infinite mass to all of the atoms excluded from the Hessian matrix. The success of this methodology relies on their being only a small coupling between the vibrational modes of the adsorbate and the vibrational modes of the surface cluster. We have recently implemented a partial Hessian methodology within the analytical frequency code of the Q-CHEM software package<sup>30</sup> and applied it to study the amide I vibration of polypeptides.<sup>31,32</sup>

In this paper, the vibrational spectroscopy of acetylene, ethylene, benzene, 1,3-butadiene, and naphthalene adsorbed on the Si(100) surface is investigated using DFT. The accuracy and computational savings of the partial Hessian approach for this problem is explored. Exploiting the reduced computational cost of this approach, the IR spectroscopy of large adsorbates in conjunction with large cluster models of the surface and the effects of surface coverage are studied.

### Computational Details

Within the harmonic approximation, vibrational frequencies and associated normal modes are obtained from the eigenvalues and eigenvectors of the Hessian matrix in mass-weighted coordinates. The Hessian matrix contains the second-derivatives of the electronic energy with respect to the nuclear coordinates, and the corresponding IR intensities are evaluated through the derivative of the dipole moment with respect to the normal coordinates. The majority of the computational effort in a harmonic frequency calculation is the evaluation of the energy

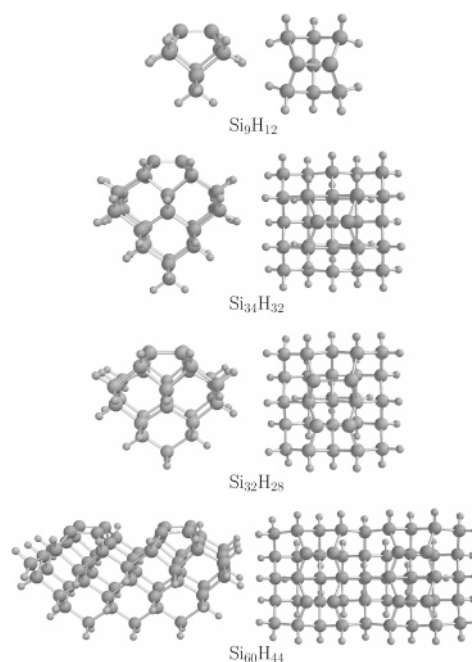


**Figure 1.** Cluster models of the Si(100) surface.

second derivatives. These derivatives can be evaluated efficiently via the coupled perturbed Hartree–Fock (or coupled perturbed Kohn–Sham) equations using the iterative procedure introduced by Pople et al.<sup>33</sup> In our current implementation within a developmental version of the Q-CHEM software, the partial Hessian approximation is exploited within the evaluation of the derivatives of the density matrix and the second derivatives of the electron repulsion integrals.<sup>31</sup>

To study the IR spectroscopy of surface adsorbates, it would be natural to truncate the Hessian matrix to include only the energy derivatives with respect to the coordinates of the atoms of the adsorbed molecule. It is important to note that these derivatives are computed for the adsorbate-molecule system, and hence the interaction with the surface is included explicitly. For the calculations presented here, except naphthalene, the derivatives with respect to the silicon atoms of the surface bonded to the adsorbate are also included within the Hessian. This is necessary to reproduce additional features of the IR spectrum, such as the Si–C stretching modes. For naphthalene, the partial Hessian is restricted to the atoms comprising naphthalene. In this work, we have used four different cluster models of the Si(100) surface which are shown in Figure 1. The  $\text{Si}_9\text{H}_{12}$  cluster is the smallest reasonable model of a single surface dimer. The larger  $\text{Si}_{34}\text{H}_{32}$  cluster provides a more substantial model of a single silicon–silicon dimer, and should provide a better model of the surface. The  $\text{Si}_{32}\text{H}_{28}$  and  $\text{Si}_{60}\text{H}_{44}$  clusters contain two and four silicon–silicon dimers and allow more aspects of the Si(100) surface chemistry to be explored. With the  $\text{Si}_{60}\text{H}_{44}$  model, surface adsorbates that bind to more than one surface dimer and multiple adsorption within and in adjacent dimers rows can be studied. While it is possible to build a four dimer cluster with less silicon atoms, we have found that including multiple layers of silicon reduces artefacts, such as curvature of the surface.<sup>6</sup> For all calculations, we have used DFT with the empirical density functional 1 (EDF1) exchange–correlations functional,<sup>34</sup> and the geometry of the cluster and adsorbate is optimized fully at the appropriate level of theory. Spectra are generated by representing each vibrational mode with a Gaussian function with full width at half-maximum of  $7.5\text{ cm}^{-1}$ . Timings correspond to a serial calculation using an Opteron 2.2 GHz processor with 2GB of memory.

**TABLE 1: Computed Vibrational Frequencies (in  $\text{cm}^{-1}$ ) and Intensities (in  $\text{km mol}^{-1}$ ) of Acetylene Adsorbed on Si(100) with Different Computational Models**

vibrational mode	full Hessian EDF1/6-31G* Si <sub>9</sub> H <sub>12</sub> cluster	partial Hessian EDF1/6-31G* Si <sub>9</sub> H <sub>12</sub> cluster	partial Hessian EDF1/mixed Si <sub>9</sub> H <sub>12</sub> cluster	partial Hessian EDF1/mixed Si <sub>34</sub> H <sub>32</sub> cluster
C–H str. <sup>a</sup>	3105.9 (73.0)	3105.9 (73.1)	3108.0 (71.7)	3114.5 (98.2)
C–H str.	3083.1 (6.2)	3083.1 (6.2)	3085.2 (5.9)	3091.4 (5.1)
C–C str.	1492.6 (0.8)	1492.5 (0.6)	1489.6 (0.2)	1484.3 (0.3)
C–H bend	1246.4 (9.5)	1246.1 (9.8)	1248.0 (9.6)	1240.2 (6.9)
C–H bend	1056.4 (4.7)	1056.3 (4.9)	1056.9 (4.5)	1049.0 (8.9)
C–H wag	966.0 (0.0)	965.3 (0.0)	967.0 (0.0)	959.7 (0.0)
Si–C str.	722.9 (0.3)	717.0 (2.1)	717.9 (2.3)	708.8 (5.1)
C–H wag	716.2 (27.6)	703.9 (99.8)	709.2 (107.0)	702.4 (86.7)
Si–C str.	697.4 (109.8)	695.8 (16.9)	696.9 (20.4)	689.7 (31.1)
Si–Si str.	436.8 (0.3)	440.7 (0.0)	439.7 (10.7)	434.6 (10.6)
time (s)	9887	5960	3601	78320

<sup>a</sup> Stretch.**TABLE 2: Computed Vibrational Frequencies (in  $\text{cm}^{-1}$ ) and Intensities (in  $\text{km mol}^{-1}$ ) of Ethylene Adsorbed on Si(100) with Different Computational Models**

vibrational mode	full Hessian EDF1/6-31G* Si <sub>9</sub> H <sub>12</sub> cluster	partial Hessian EDF1/6-31G* Si <sub>9</sub> H <sub>12</sub> cluster	partial Hessian EDF1/mixed Si <sub>9</sub> H <sub>12</sub> cluster	partial Hessian EDF1/mixed Si <sub>34</sub> H <sub>32</sub> cluster
C–H str. <sup>a</sup>	3093.6 (6.7)	3093.6 (6.7)	3094.1 (6.5)	3102.9 (4.5)
C–H str.	3074.2 (4.8)	3074.2 (4.8)	3074.5 (4.3)	3082.1 (0.1)
C–H str.	3034.4 (33.5)	3034.4 (33.4)	3035.0 (31.5)	3043.1 (36.8)
C–H str.	3026.4 (11.2)	3026.4 (11.1)	3026.7 (10.8)	3033.0 (8.1)
CH <sub>2</sub> bend	1457.4 (0.7)	1457.7 (0.6)	1455.7 (0.8)	1446.2 (0.8)
CH <sub>2</sub> bend	1443.4 (2.6)	1443.4 (2.7)	1440.8 (2.4)	1438.4 (0.1)
C–H wag	1216.5 (1.0)	1216.3 (1.1)	1213.4 (0.9)	1216.7 (0.0)
CH <sub>2</sub> rock	1169.7 (1.9)	1169.4 (1.9)	1168.2 (1.7)	1164.6 (2.1)
CH <sub>2</sub> rock	1112.2 (0.1)	1112.1 (0.2)	1110.0 (0.0)	1116.4 (0.8)
C–H wag	1017.2 (15.0)	1015.7 (11.2)	1012.8 (11.8)	1018.2 (9.7)
C–C str.	932.2 (1.1)	931.6 (0.2)	927.4 (0.3)	925.1 (0.5)
CH <sub>2</sub> rock	763.2 (1.7)	749.0 (2.0)	746.5 (1.8)	736.4 (0.0)
C–Si str.	697.6 (3.3)	692.5 (11.8)	689.3 (11.7)	655.0 (9.0)
C–Si str.	657.6 (45.1)	642.1 (20.6)	643.1 (11.7)	630.2 (35.9)
Si–Si str.	442.9 (1.2)	452.9 (0.4)	472.0 (0.2)	455.9 (2.9)
time (s)	11525	7123	4514	84363

<sup>a</sup> Stretch.

## Results and Discussion

**Acetylene and Ethylene.** Acetylene and ethylene adsorbed on the surface provide suitable models to explore different computational models to study the vibrational modes of the surface adsorbed species. Table 1 shows the computed vibrational frequencies and intensities of acetylene adsorbed on the surface. Also shown are the Si–C stretching modes and Si–Si stretch of the two silicon atoms bonded to acetylene. The EDF1/6-31G\* calculation with the full Hessian represents a typical calculation that is used to study this problem. For acetylene, the partial Hessian approximation introduces only a small error in the vibrational frequencies and intensities. The typical error in the computed frequencies is less than  $1 \text{ cm}^{-1}$  and less than  $0.5 \text{ km mol}^{-1}$  for the intensities. In particular, the C–H stretching frequencies and intensities are virtually unaffected. The success of the partial Hessian approximation relies on there being only a small coupling with the motion of the surface atoms. One of the reasons for this weak coupling is the large difference in mass of the atoms of the adsorbate and the surface. The exception is the symmetric C–H wag where a larger error in the frequency and intensity is observed. This is a consequence of this vibrational mode being coupled to a motion of the whole cluster. The inclusion of the two surface silicon atoms within the partial Hessian leads to a reasonable description of the Si–C and Si–Si stretching modes.

Even for this relatively small system, the computational savings are significant, and the time for the calculation is reduced

by approximately 40%. To reduce the cost of the calculation further, a mixed basis set comprising the 6-31G\* basis set for the atoms of acetylene and the two surface silicon atoms bonded to acetylene and the 6-31G basis set for the remainder of the surface atoms was used. This basis set is denoted ‘mixed’ in Table 1. Such mixed basis sets have been used in previous studies.<sup>16</sup> Before the frequency calculation, the geometry is optimized fully with the mixed basis set. The resulting frequencies and intensities are in good agreement with the full 6-31G\* basis set and there is a further significant reduction in the cost of the calculation. Using the partial Hessian in conjunction with the mixed basis set, the vibrational frequencies of acetylene on the larger single dimer cluster model can be computed. The resultant spectrum is similar to the corresponding calculation with the mixed basis set on the smaller cluster, with about a  $10 \text{ cm}^{-1}$  difference in the vibrational frequencies. For the larger cluster model, the vibrational frequencies are lower for all vibrational modes except the C–H stretches. However, the smaller cluster model does provide a good model of the adsorption of a single acetylene molecule.

Table 2 shows computed frequencies and intensities of ethylene adsorbed on the surface. The calculations follow a similar pattern to acetylene. The vibrational frequencies of the adsorbed ethylene molecule within the partial Hessian approximation are very close to the full Hessian values. Some larger errors are observed for the lower frequency modes, including the C–Si and Si–Si stretches, but these are repro-

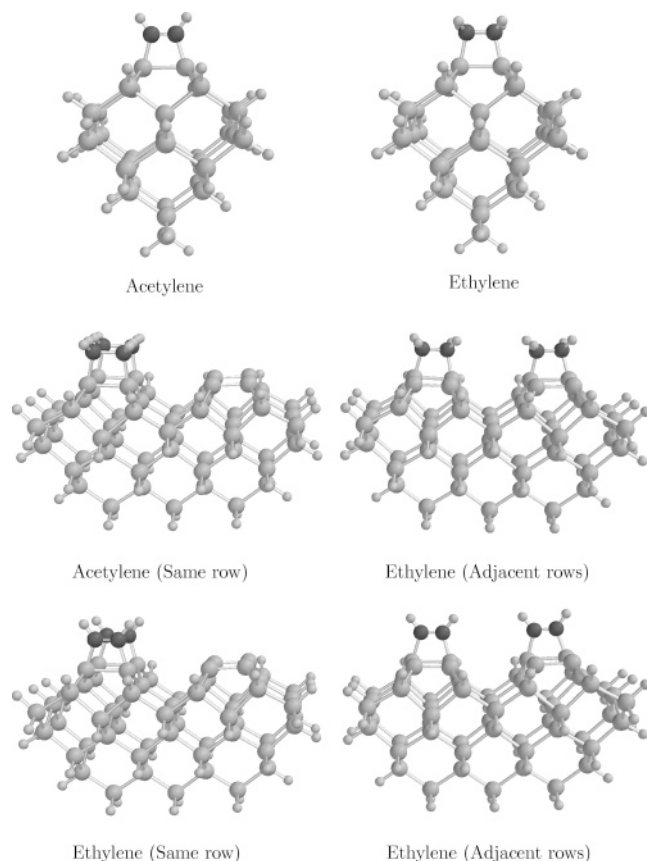
**TABLE 3: C–H Stretching Frequencies (in  $\text{cm}^{-1}$ ) and Intensities ( $\text{km mol}^{-1}$ ) for Two Acetylene, Ethylene, or Benzene Molecules Adsorbed on the Same or Adjacent Dimer Rows of the  $\text{Si}_{60}\text{H}_{44}$  Surface Cluster Model<sup>a</sup>**

	same dimer row	adjacent dimer row	
acetylene	3114.2 (78.8)	3114.8 (57.5)	
	3110.2 (54.4)	3113.2 (66.1)	
	3090.5 (4.8)	3091.8 (2.9)	
	3087.1 (4.8)	3090.3 (3.5)	
ethylene	3110.5 (3.9)	3105.6 (6.8)	
	3105.4 (4.8)	3105.3 (3.2)	
	3090.0 (3.1)	3084.7 (0.5)	
	3083.8 (0.6)	3084.2 (0.1)	
	3050.6 (23.9)	3043.7 (26.0)	
	3045.9 (26.2)	3042.1 (17.5)	
	3039.9 (11.0)	3034.0 (3.9)	
	3033.0 (5.7)	3032.9 (9.4)	
	benzene	3080.5 (31.9)	3057.5 (6.0)
		3071.0 (2.1)	3056.6 (8.6)
3064.3 (11.9)		3054.4 (15.7)	
3064.0 (9.6)		3054.0 (17.2)	
3058.5 (5.5)		3036.3 (1.5)	
3051.1 (1.8)		3035.4 (0.3)	
3044.8 (1.0)		3034.5 (1.2)	
3044.3 (0.2)		3033.8 (1.6)	
2964.4 (1.0)		2965.4 (1.9)	
2962.0 (0.3)		2963.5 (5.1)	
2959.1 (5.5)	2959.9 (4.6)		
2956.0 (4.9)	2956.8 (7.3)		

<sup>a</sup> Frequencies for benzene have been scaled by 0.96.

duced reasonably well. Using the 6-31G basis set for the atoms of the cluster not bonded to ethylene introduces an additional small error of a few wavenumbers. Overall the partial Hessian calculation with mixed basis set reduces the time for the calculation by over 60%. Using the larger single dimer cluster, the computed frequencies are in close agreement with the  $\text{Si}_9\text{H}_{12}$  cluster. The largest differences are observed for C–H stretching modes, which differ by between 5 and 10  $\text{cm}^{-1}$ . These calculations on acetylene and ethylene demonstrate that the partial Hessian approximation can reduce the cost of the calculations while only introducing a small error in the computed vibrational properties. However, to assess the applicability of the partial Hessian approximation, in principle, requires a full Hessian calculation. Strategies to test the validity of a partial Hessian model can be employed that avoid the need for an expensive full Hessian calculation. These include checking the invariance of the computed frequencies after a small increase in the size of the Hessian matrix or comparing full and partial Hessian calculations using a small or minimal basis set. In the partial Hessian implementation of Head,<sup>27</sup> a diagnostic to estimate the coupling and hence the validity of a partial Hessian approach between the adsorbate and cluster atoms was developed.

The reduced cost of the calculations makes the study of molecules adsorbed on the large four dimer cluster tractable. Using this cluster, it is possible to study more than one molecule adsorbed on the surface. Since experiments measure the C–H stretching frequencies, we will focus on these vibrational modes. Table 3 shows the computed C–H stretching frequencies of two acetylene or ethylene molecules adsorbed on adjacent dimers in the *same* dimer row and in *adjacent* dimer rows. The adsorbed molecules are shown in Figure 2. Molecules adsorbed in adjacent dimer rows are further apart than those adsorbed in the same dimer row, and this is evident in the computed vibrational frequencies. For both acetylene and ethylene, there is little splitting in the vibrational modes when the two molecules are adsorbed in different dimer rows. However, even these small

**Figure 2.** Models of acetylene and ethylene adsorbed on Si(100).

molecules adsorbed in the same dimer row show a change in the vibrational frequencies. A splitting of 5–10  $\text{cm}^{-1}$  in corresponding vibrational modes is observed for ethylene, with a slightly smaller splitting for acetylene.

**Benzene.** The adsorption of benzene on Si(100) has been studied extensively, and experimental spectra of the C–H stretching region have been reported. For benzene chemisorbed at 300 K, the spectrum reported by Kong et al. showed two peaks at 3044 and 2945  $\text{cm}^{-1}$ .<sup>14</sup> After annealing to 350 K the peak at 2945  $\text{cm}^{-1}$  was absent and an additional peak at 2899  $\text{cm}^{-1}$  is observed. In both spectra, the peak at 3044  $\text{cm}^{-1}$  is more intense. The spectrum of Lopinski et al. is reproduced in Figure 3, and has four peaks at 3045, 2947, 2921, and 2901  $\text{cm}^{-1}$ . Figure 3 also shows spectra computed using the  $\text{Si}_{34}\text{H}_{32}$  cluster and mixed basis set for the [4+2] and [2+2] addition products. These binding configurations are illustrated in Figure 4. The computed frequencies have been scaled by 0.96 to agree with experiment. For the [4+2] product, the calculations predict two intense peaks at 3052 and 2958  $\text{cm}^{-1}$ . The peak at lower wavenumber arises from the C–H stretches of the  $\text{sp}^3$  hybridized carbons bonded to the surface, while the peak at higher wavenumber corresponds to the  $\text{sp}^2$  hybridized carbons. These peaks are clearly evident in experiment, indicating that the [4+2] adsorbed species is present. The spectrum for the [2+2] addition has a similar intense peak at 3037  $\text{cm}^{-1}$  arising from the hydrogens of the  $\text{sp}^2$  carbons. However, the C–H stretches for the  $\text{sp}^3$  hybridized carbons bonded to the surface appear at 2876 and 2897  $\text{cm}^{-1}$ , a lower frequency than the corresponding modes of the [4+2] addition product. One possible origin of this difference is the carbons bonded to the surface are more distorted from an ideal  $\text{sp}^3$  hybridized carbon in the [2+2] product. The experiment does show peaks in the 2900  $\text{cm}^{-1}$  region suggesting the [2+2] product may be present. The [2+2] product cannot account for the greater intensity of the experimental bands in

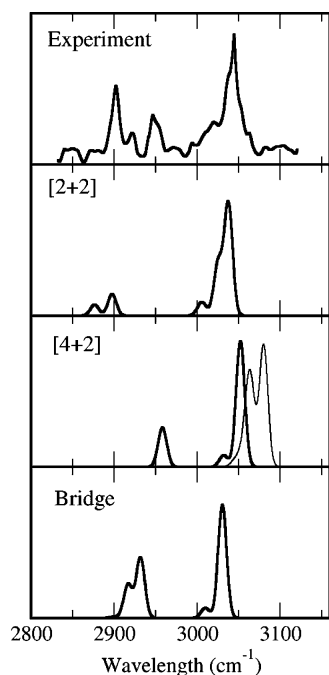


**Figure 3.** Computed spectra for the C–H stretches of benzene adsorbed in the [2+2] and [4+2] configurations on the  $\text{Si}_{34}\text{H}_{32}$  cluster. Narrow line: computed spectra for two benzene molecules in the [4+2] configuration adsorbed on adjacent silicon dimers in the same dimer row. Experimental spectrum is adapted from ref 18.

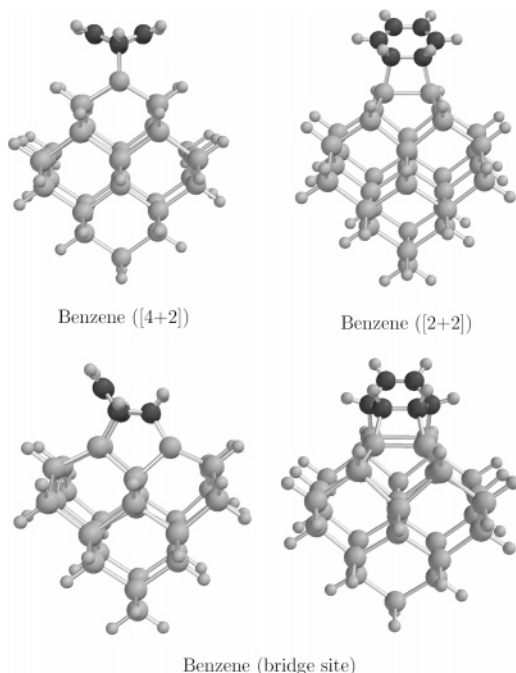


**Figure 4.** Models of benzene adsorbed on  $\text{Si}(100)$ .

this region, indicating that other adsorption products are present. Also shown is the computed spectrum for benzene adsorbed in a “bridge” site where it is bonded to two silicon–silicon dimers within the same dimer row as shown in Figure 4. In this binding geometry the C–H stretching bands occur at 3031, 2932, and 2916  $\text{cm}^{-1}$ . The spectrum for this bonding configuration does have bands that agree relatively well with the experimental bands at 2901 and 2921  $\text{cm}^{-1}$ . This indicates that this absorption product is also present. A combination of the [4+2] and bridge products can account for the major features observed in experiment. These two binding configurations are predicted to have a greater binding energy than the [2+2] product.<sup>6</sup> However,

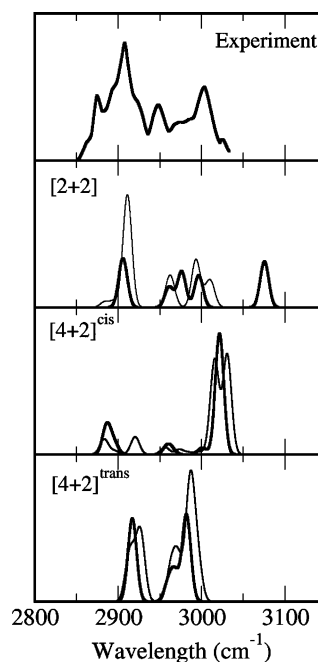


**Figure 5.** Computed spectra for the C–H stretches of 1,3-butadiene adsorbed on the  $\text{Si}_{34}\text{H}_{32}$  cluster. Narrow lines: computed spectra for two butadiene molecules adsorbed on adjacent silicon dimers in the same dimer row on the  $\text{Si}_{60}\text{H}_{44}$  cluster. Experimental spectrum is adapted from ref 13.

it is not possible to exclude the possibility of other adsorption products. These calculations agree with earlier semiempirical and DFT calculations on this system.<sup>18</sup>

Table 3 shows the computed C–H stretching frequencies for two benzene molecules adsorbed on the surface in the [4+2] configuration. When the two benzene molecules are adsorbed on silicon dimers in adjacent dimer rows, there is little change in the frequencies and intensities. However, when two benzene molecules are adsorbed on adjacent dimers in the same dimer row there are significant changes. The resulting spectrum is shown in Figure 3. The lower wavenumber band is not affected by the neighboring molecule. This is physically reasonable since this band arises from the hydrogens of the  $\text{sp}^3$  carbons bonded to the surface and do not point in the direction of the neighboring benzene. The band at higher wavenumber corresponds to the hydrogens bonded to the  $\text{sp}^2$  carbons. These hydrogens will be close to the equivalent hydrogens of the neighboring benzene molecule. This is reflected in the resultant spectral band, which shows two distinct peaks that are shifted by 20–30  $\text{cm}^{-1}$ . Overall, while the computed spectrum is changed by the presence of additional molecules adsorbed on neighboring sites, the resulting spectrum remains consistent with the established interpretation of the experimental spectrum. A closer observation of the computed spectra shows that the computed spectrum for the singly adsorbed product is in better agreement with experiment. This indicates that benzene molecules may not be adsorbed on neighboring sites within a dimer row. However, the accuracy of the calculations makes analysis of the results at this level quite tentative.

**1,3-Butadiene.** Figure 5 shows the experimental spectrum for the C–H stretching region for 1,3-butadiene adsorbed on the surface. The experiment has distinct bands at approximately 2905, 2950, and 3000  $\text{cm}^{-1}$ .<sup>13</sup> Spectra recorded using deuterated butadiene showed that the structure resulting from the [4+2] addition is dominant. DFT calculations predicted vibrational frequencies of the [4+2] structure that were in good agreement with experiment. For the [2+2] structure, a band at 3054  $\text{cm}^{-1}$

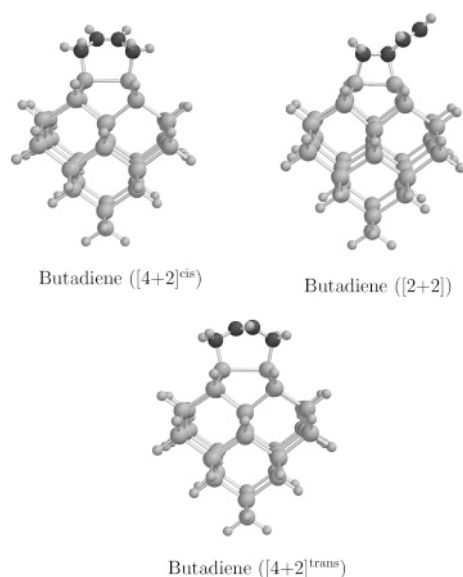


**Figure 6.** Models of 1,3-butadiene adsorbed on Si(100).

corresponding to vinylic  $\text{CH}_2$  was predicted, which is not observed in the experimental spectrum. These results were consistent with the [4+2] structure being preferred.

IR spectra have been computed for three adsorption configurations on the  $\text{Si}_{34}\text{H}_{32}$  cluster, the resulting spectra (scaled by 0.96) are shown in Figure 5. These include the [2+2] structure and two structures arising from a [4+2] addition shown in Figure 6. In these two structures, the hydrogens of the  $\text{sp}^2$  carbons are either cis or trans. For the [2+2] structure, spectral bands at 2905, 2961, 2996, 3009, and 3075  $\text{cm}^{-1}$  are predicted. The bands at 2905 and 2961  $\text{cm}^{-1}$  arise from the hydrogens bonded to the  $\text{sp}^3$  carbons, and the bands at higher wavelength arise from the hydrogens bonded to the carbons not attached to the surface. The four lowest of these bands correspond well to spectral bands observed in the experiment. The exception is the band at 3075  $\text{cm}^{-1}$ , which is not present in experiment. This band provides theoretical evidence for the [2+2] addition product not being present.<sup>21</sup>

The [4+2] structure in which the hydrogens are cis corresponds to the structure considered in earlier work.<sup>21,22</sup> For this structure, the computed vibrational frequencies correspond well to spectral bands seen in experiment. However, the computed intensities do not agree well, and the resulting spectrum does not reproduce experiment well. In particular, the lower wavelength bands are too weak relative to the band at 3021  $\text{cm}^{-1}$ . The structure resulting from a [4+2] addition is one in which the hydrogens bonded to the  $\text{sp}^2$  carbons are trans with respect to each other, and the computed spectrum has two intense bands at 2916 and 2980  $\text{cm}^{-1}$ . These agree well with the lower wavelength bands observed in experiment, and a combination of cis and trans products could reproduce the experimental spectrum well and be consistent with the isotopically labeled spectra. This suggests that both cis and trans [4+2] adsorption products may be present even though the trans product is computed to be higher in energy. Also shown are spectra computed when two butadiene molecules are adsorbed on adjacent dimers in the same dimer row. The presence of molecule adsorbed on a neighboring dimer does affect the spectra. In particular, the spectrum for the [2+2] addition product changes significantly. The band at 2905  $\text{cm}^{-1}$  increases its intensity; however, crucially the band at 3075  $\text{cm}^{-1}$  is not affected. For the cis and trans [4+2] adsorption products, the computed spectra are qualitatively similar.

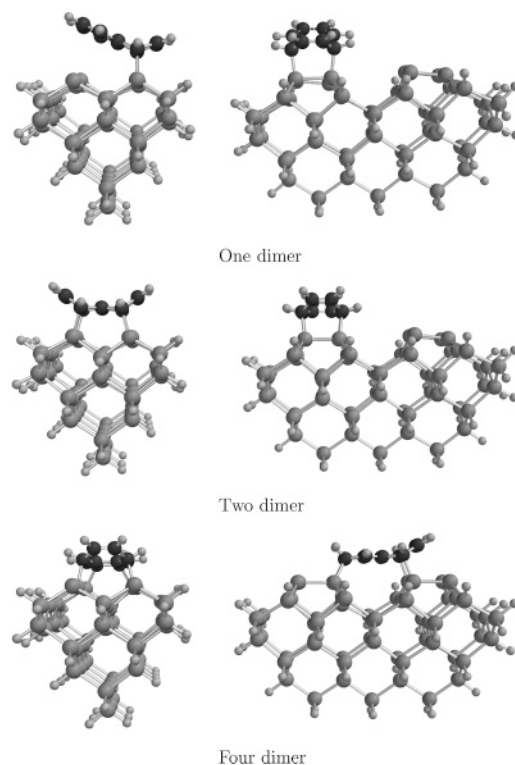


**Figure 7.** Models of naphthalene adsorbed on Si(100).

Overall, the adsorption of the relatively simple molecule 1,3-butadiene presents a fairly complex picture. Experimental studies of isotopically labeled molecules indicate clearly that the main adsorption product is from the [4+2] addition. The theoretical calculations are consistent with this observation. The cis [4+2] product has an intense band at 3021  $\text{cm}^{-1}$ , and this corresponds to a spectral band present in experiment. However, this adsorption product cannot account for the other bands observed. Our calculations suggest that the trans [4+2] adsorption product these bands can be account for these bands.

**Naphthalene.** Naphthalene is a large adsorbate and can adopt a range of adsorption configurations, including adsorption between dimer rows. IR spectra for naphthalene adsorbed in three binding configurations corresponding to bonding to one, two and four silicon dimers have been computed. These structures are shown in Figure 7. The one and two dimer adsorption products correspond to the tilted and symmetric bridge structures studied in earlier work.<sup>20</sup> Figure 8 shows the computed spectra for the C–H stretching region with the experimental spectrum measured at low coverage.<sup>20</sup> Experiment shows an intense peak at about 3050  $\text{cm}^{-1}$  and a weaker peak at 2950  $\text{cm}^{-1}$ . The computed spectra for naphthalene bonded to one and two silicon dimers agree well with the experimental spectrum. Both configurations have an intense band close to 3050  $\text{cm}^{-1}$ , arising from the  $\text{sp}^2$  carbons, with weaker bands at 2950  $\text{cm}^{-1}$ . Based on the computed spectra both configurations could be present, although the single bond configuration is predicted to be higher in energy.<sup>20</sup> Also shown is the spectrum computed for naphthalene bonded to four silicon dimers. This adsorption configuration involves both [2+2] and [4+2] adsorption to the surface. The computed spectrum for this configuration differs significantly from experiment. In particular, a band at 2910  $\text{cm}^{-1}$  is not observed in experiment suggesting that this configuration is not present with significant abundance at low coverage.

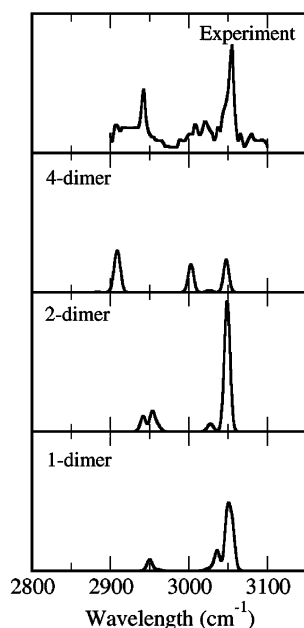


**Figure 8.** Computed spectra for the C–H stretches of naphthalene on the  $\text{Si}_{60}\text{H}_{44}$  cluster. Experimental spectrum is adapted from ref 20.

### Conclusions

DFT calculations of the IR spectroscopy of molecules adsorbed on surfaces in conjunction with experimental measurements can provide a valuable approach to probe the structure of an adsorbed molecule. In this paper, we exploit a partial Hessian approach in conjunction with a reduced basis set for the surface atoms to reduce the cost of the calculations while introducing only a small error in the computed frequencies and intensities. Using this methodology, the study of large cluster models is computationally tractable.

In this work, we have focused on organic molecules adsorbed on the Si(100) surface. For small adsorbates, the single dimer  $\text{Si}_9\text{H}_{12}$  cluster is an efficient model of the surface. Computed spectra with this cluster are quantitatively similar to those computed with large cluster models, and the differences in the computed vibrational frequencies are less than other errors inherent in the calculations. However, to model the adsorption of larger adsorbates and the effects of surface coverage, larger cluster models of the surface are required. For the molecules studied, the presence of a similar molecule in an adjacent dimer row has little effect on the vibration modes. However, the adsorption of a molecule on an adjacent silicon dimer in the same dimer row did have a greater effect on the computed vibrational frequencies and intensities. In particular, for benzene and butadiene, the resultant spectra changed significantly.

For benzene, the results of the calculations presented here agree well with previous semiempirical AM1 calculations,<sup>18</sup> indicating that benzene adopts several binding configurations. For 1,3-butadiene the results are consistent with experiment and previous theoretical studies that find the [4+2] product to be the dominant species. However, to account for all of the bands observed in experiment, our calculations show that it is necessary to consider two products of the [4+2] addition in which the hydrogens of the  $\text{sp}^2$  carbons are cis or trans. Naphthalene can bind to multiple silicon dimers on the surface and possibly between dimer rows. The calculations show at low

coverage this binding occurs within a dimer row and binding between adjacent dimer rows does not occur with a large abundance.

**Acknowledgment.** N.A.B. is grateful to the Engineering and Physical Sciences Research Council (U.K.) for the award of an Advanced Research Fellowship (GR/R77636) and to the University of Nottingham for access to its High Performance Computing facility.

### References and Notes

- (1) Bent, S. F. *Surf. Sci.* **2002**, *500*, 879.
- (2) McEllistrem, M.; Allgeier, M.; Boland, J. J. *Science* **1998**, *279*, 545.
- (3) Buehler, E. J.; Boland, J. J. *Science* **2000**, *290*, 506.
- (4) Lopinski, G. P.; Wayner, D. D. M.; Wolkow, R. A. *Nature* **2000**, *406*, 48.
- (5) Ho Choi, C.; Gordon, M. S. *J. Am. Chem. Soc.* **2002**, *124*, 6162.
- (6) Phillips, M. A.; Besley, N. A.; Gill, P. M. W.; Moriarty, P. *Phys. Rev. B* **2003**, *67*, 035309.
- (7) Rintelman, J. M.; Gordon, M. S. *J. Phys. Chem. B* **2004**, *108*, 7820.
- (8) Jung, Y.; Gordon, M. S. *J. Am. Chem. Soc.* **2005**, *127*, 3131.
- (9) Besley, N. A. *Chem. Phys. Lett.* **2004**, *390*, 124.
- (10) Besley, N. A. *J. Chem. Phys.* **2005**, *122*, 184706.
- (11) Besley, N. A.; Blundy, A. J. *J. Phys. Chem. B* **2006**, *110*, 1701.
- (12) Besley, N. A.; Noble, A. *J. Phys. Chem. C* **2007**, *111*, 3333.
- (13) Teplyakov, A. V.; Kong, M. J.; Bent, S. F. *J. Am. Chem. Soc.* **1997**, *119*, 11100.
- (14) Kong, M. J.; Teplyakov, A. V.; Lyubovitsky, J. G.; Bent, S. F. *Surf. Sci.* **1998**, *411*, 286.
- (15) Teplyakov, A. V.; Kong, M. J.; Bent, S. F. *J. Chem. Phys.* **1998**, *108*, 4599.
- (16) Mui, C.; Wang, G. T.; Bent, S. F.; Musgrave, C. B. *J. Chem. Phys.* **2001**, *114*, 10170.
- (17) Taguchi, Y.; Fujisawa, M.; Takoka, T.; Okada, T.; Nishijima, M. *J. Chem. Phys.* **1991**, *95*, 6870.
- (18) Lopinski, G. P.; Fortier, T. M.; Moffatt, D. J.; Wolkow, R. A. *J. Vac. Sci. Technol.* **1998**, *16*, 1037.
- (19) Hovis, J. S.; Liu, H.; Hamers, R. J. *J. Phys. Chem. B* **1998**, *102*, 6873.
- (20) Okamura, K.; Ishii, H.; Kimuar, Y.; Niwano, M. *Surf. Sci.* **2005**, *576*, 45.
- (21) Konecny, R.; Doren, D. J. *J. Am. Chem. Soc.* **1997**, *119*, 11098.
- (22) Konecny, R.; Doren, D. J. *Surf. Sci.* **1998**, *417*, 169.
- (23) Wang, G. T.; Mui, C.; Musgrave, C. B.; Bent, S. F. *J. Phys. Chem. B* **1999**, *103*, 6803.
- (24) Nicholson, K. T.; Banaszak Holl, M. M. *Phys. Rev. B* **2001**, *64*, 155317.
- (25) Herrmann, C.; Reiher, M. *Surf. Sci.* **2006**, *600*, 1891.
- (26) Reiher, M.; Neugebauer, J. *J. Chem. Phys.* **2003**, *118*, 1634.
- (27) Head, J. D. *Int. J. Quantum Chem.* **1997**, *65*, 827.
- (28) Head, J. D.; Shi, Y. *Int. J. Quantum Chem.* **1999**, *75*, 815.
- (29) Head, J. D. *Int. J. Quantum Chem.* **2000**, *77*, 350.
- (30) Shao, Y.; Molnar, L. F.; Jung, Y.; Kussmann, J.; Ochsenfeld, C.; Brown, S. T.; Gilbert, A. T. B.; Slipchenko, L. V.; Levchenko, S. V.; O'Neill, D. P.; DiStasio, R. A.; Lochan, R. C.; Wang, T.; Beran, G. J. O.; Besley, N. A.; Herbert, J. M.; Lin, C. Y.; Van Voorhis, T.; Chien, S. H.; Sodt, A.; Steele, R. P.; Rassolov, V. A.; Maslen, P. E.; Korambath, P. P.; Adamson, R. D.; Austin, B.; Baker, J.; Byrd, E. F. C.; Dachsel, H.; Doerksen, R. J.; Dreuw, A.; Dunietz, B. D.; Dutoi, A. D.; Furlani, T. R.; Gwaltney, S. R.; Heyden, A.; Hirata, S.; Hsu, C. P.; Kedziora, G. S.; Khalliulin, R. Z.; Klunzinger, P.; Lee, A. M.; Lee, M. S.; Liang, W.; Lotan, I.; Nair, N.; Peters, B.; Proynov, E. I.; Pieniazek, P. A.; Rhee, Y. M.; Ritchie, J.; Rosta, E.; Sherrill, C. D.; Simmonett, A. C.; Subotnik, J. E.; Woodcock, H. L., III; Zhang, W.; Bell, A. T.; Chakraborty, A. K.; Chipman, D. M.; Keil, F. J.; Warshel, A.; Hehre, W. J.; Schaefer, III, H. F.; Kong, J.; Krylov, A. I.; Gill, P. M. W.; Head-Gordon, M. *Phys. Chem. Chem. Phys.* **2006**, *8*, 3172.
- (31) Besley, N. A.; Metcalf, K. A. *J. Chem. Phys.* **2007**, *126*, 035101.
- (32) Besley, N. A. *Phil. Trans. R. Soc. A* **2007**, *365*, 2799.
- (33) Pople, J. A.; Krishnan, R.; Schlegel, H. B.; Binkley, J. S. *Int. J. Quantum Chem. Symp.* **1979**, *13*, 225.
- (34) Adamson, R. D.; Gill, P. M. W.; Pople, J. A. *Chem. Phys. Lett.* **1998**, *284*, 6.